Liquid Crystals
Publication details, including instructions for authors and subscription information:
http://www.informaworld.com/smpp/title~content=t713926090

Advanced wide viewing angle technology in liquid crystal display modes

Seung-Hoon Ji[a]; Gi-Dong Lee[a]
[a] Department of Electronics Engineering, Dong-A University, Pusan, Korea

To cite this Article Ji, Seung-Hoon and Lee, Gi-Dong(2009) 'Advanced wide viewing angle technology in liquid crystal display modes', Liquid Crystals, 36: 6, 657 — 668
To link to this Article: DOI: 10.1080/02678290902755580
URL: http://dx.doi.org/10.1080/02678290902755580

Liquid Crystals,
Vol. 36, Nos. 6–7, June–July 2009, 657–668

Taylor & Francis
Taylor & Francis Group

INVITED ARTICLE

Advanced wide viewing angle technology in liquid crystal display modes

Seung-Hoon Ji and Gi-Dong Lee*

Department of Electronics Engineering, Dong-A University, Pusan 604-714, Korea

(Received 31 December 2008; accepted 16 January 2009)

This paper reviews the advanced optical configurations for in-plane switching (IPS) and vertical alignment (VA) liquid crystal (LC) cells with wide viewing angle in a visible wavelength range. Optical compensation and optimisation to eliminate off-axis light leakage in the dark state is performed on a Poincaré sphere using the trigonometric and the Muller matrix method. By optimising the wavelength dispersion of used optical retardation films, we could achieve wide-view characteristics for both the IPS and VA LC cells. In addition, we show the advanced wide-view technology for a reflective LC mode.

Keywords: liquid crystal; optical configuration; wide viewing angle; Poincaré sphere

1. Introduction

Transmissive liquid crystal displays (LCDs) are being widely used due to their high resolution, wide viewing angle and fast response time. Reflective LCDs can be applied to mobile display devices because of their lower power consumption and light weight. To meet the optical requirements, horizontal switching LC modes including in-plane switching (IPS) (*1*) and fringe-field switching (FFS) (*2*), and vertical switching LC modes such as patterned vertical alignment (PVA) (*3*) and multi-domain vertical alignment (MVA) (*4*) have been developed. In spite of these efforts, LCD image quality is still insufficient for large-screen products when applying the LC mode alone, because of the narrow viewing angle compared with the emissive display device. A single-polariser mode is considered a suitable structure for reflective LC cells as it shows greater brightness than the double-polariser mode such as the transmissive LCDs (*5, 6*). However, the LC modes have a common problem of lower contrast due to the off-axis light leakage in the dark state as the optical performance of the LCD is strongly affected by optical films such as polarisers and retardation films (*7*).

Recently, the property of a wide viewing angle has become an important requirement for high image quality LCDs such as televisions and large-screen desktop monitors, and also mobile display devices. In this paper, we introduce the advanced transmissive and reflective IPS and VA LC modes, which can optically show wide viewing angle characteristics by compensating for off-axis light leakage in the dark state in the visible wavelength range.

2. Off-axis light leakage in the dark state

There are several reasons for light leakage of the LC mode in the diagonal direction with oblique incidence. An important reason for light leakage is the movement of the polarisation axis of the crossed polarisers, which increases with the polar angle of the observation angle in the diagonal direction. Thus, the effective principle axis of the optical components deviates from the principle axis in the normal incidence by angle δ. In terms of the polarisers, if we apply the very small birefringence approximation ($n_e \approx n_o$), the deviation of the azimuth angle δ from δ_o can be described as (*8*):

$$\sin(\delta - \delta o) = -\frac{\sin 2\phi_c \sin^2(\theta_o/2)}{\sqrt{1 - (\sin\phi_c \sin\theta_o)^2}}, \quad (1)$$

where ϕ_c is the azimuth angle of the polarisation axis of the polariser, and θ_o is the polar angle of the incident light in the LC layer. n_e and n_o represent the extraordinary and the ordinary refractive index of the polariser and retardation film, respectively. δ_o represents the angle between the polarisation axis of the polariser and the x-axis at normal direction. From Equation (1), the deviation angle $\Delta\delta$ (= $\delta - \delta_o$) is maximised in the diagonal direction ($\phi = 45°$). Regarding the optical axis of the optical film, the effective angle of the optical axis of the retarder in the oblique incidence is changed as a function of the observation angle. The effective optical axis of the *A*-plate is also derived through Equation (1). Thus, the optical axis of the *A*-plate moves as much as the

*Corresponding author. Email: gdlee@dau.ac.kr

ISSN 0267-8292 print/ISSN 1366-5855 online

DOI: 10.1080/02678290902755580
http://www.informaworld.com

deviation angle $\Delta\delta$ from the optical axis in the normal incidence. In the case of the *C*-plate and VA LC cell, the effective fast or slow axis moves to 90° with respect to the projected angle of the incident *k* vector.

The second factor is a change in the retardation value of the compensation film in the oblique incidence. The effective retardation of the *A*-plate, *C*-plate and VA LC cell in the oblique incident angle can be described as (*8–10*):

$$\Gamma_A = \frac{2\pi}{\lambda} d \left[n_e \left(1 - \frac{\sin^2\theta \sin^2\phi}{{n_e}^2} - \frac{\sin^2\theta \cos^2\phi}{{n_o}^2} \right)^{1/2} - n_o \left(1 - \frac{\sin^2\theta}{{n_o}^2} \right)^{1/2} \right], \quad (2)$$

$$\Gamma_C = \frac{2\pi}{\lambda} n_o d \left(\sqrt{1 - \frac{\sin^2\theta}{n_e^2}} - \sqrt{1 - \frac{\sin^2\theta}{n_o^2}} \right), \quad (3)$$

where Γ_A and Γ_C represent the phase retardation of the *A*-plate and the *C*-plate at the oblique incidence, respectively. θ represents the polar angle of the incident light in free space and ϕ is the azimuth angle of the incident angle. *d* represents the thickness of the film, and λ represents the wavelength of the incident light.

The last issue is the dispersion of the refractive index of the optical components along the wavelength (*11*). In general, dispersion is also dependent on material property. The polarisation states of the three primary colours (*R*, *G*, and *B*) usually differ from each other after passing through the LC cell and the retardation films because of the different material and wavelength dispersion properties. Therefore, to minimise light leakage at the oblique incidence in the dark state, the phase dispersion in the entire visible wavelength should be eliminated.

3. Transmissive in-plane switching liquid crystal mode

3.1 Polarisation states for the conventional transmissive IPS LC cell

The conventional IPS cell consists of a homogeneous LC cell and two tri-acetyl-cellulose (TAC) films on upper and lower polarisers as shown in Figure 1(a) (12). Figure 1(b) shows the polarisation state of the light obliquely passing through the cell in the diagonal direction on the Poincaré sphere (*12–15*). Oblique incident light in the diagonal direction will have a deviated polarisation angle δ compared with normal incident light, so that the polarisation position of the polariser will deviate with 2δ from S_1, which is the polarisation state of the polariser in a normal direction. Therefore, the start position of the oblique incident light is position *A*. Then polarisation of the light will move to position *D* by experiencing two TAC films and a LC cell. The circle path L_1, L_2 and L_3 represents the polarisation paths when the light passes through each optical component, that is, a lower TAC film, an LC cell and an upper TAC film, in turn. Here, polarisation position *D* is quite different from polarisation position *G*, which is the perfect opponent position of the polarisation axis of the analyser in the oblique incidence. We can assume that the deviation between *D* and *G* will cause serious light leakage in the dark state (*12*).

Figure 1(c) represents the calculated polarisation of the *R* (633 nm), *G* (546 nm) and *B* (436 nm) wavelengths of light in front of the output polariser at $\phi = 45°$, $\theta = 70°$, and the symbols •, ■, ◆ represent the polarisation state of the light with the red, green, and blue wavelengths, respectively.

Figure 1(d) represents the measured iso-contrast of the conventional LC cell, which exhibits a very narrow viewing angle, especially, in the diagonal direction (*12*).

3.2 Advanced optical configuration using two A-plates and one C-plate for the transmissive IPS LC cell

Figure 2(a) shows the advanced optical configuration for the horizontal-switching cell, which has TAC films with retardation (*12*). The optical configuration of the advanced LC cell consists of two *A*-plates, a +*C* plate and a horizontal-switching cell. The optical axis of lower *A*-plate and horizontal-switching cell is aligned parallel with the absorption axis of the incident polariser. The optical axis of the upper *A*-plate is aligned along that of the absorption axis of the analyser. The polarisation path of the advanced LC cell is described on the Poincaré sphere as shown in Figure 2(b) (*12*). Optimisation of the optical configuration has been performed at the diagonal direction, because the light leakage in the dark state is maximised at $\phi = 45°$.

The optical principle of the optical compensation for wide viewing angle is as follows. The polarisation state in front of the output polariser can be coincided with the absorption axis of the output polariser through five paths (L_1 to L_5). The polarisation of light passing through the lower *A*-plate and the horizontal-switching cell moves to position *D* along the circle path L_1 and L_2. The polarisation of the light approaches the position *G* along the circle path L_3, which is centred at point *J* because the optical axis of the upper *A*-plate is aligned parallel with the absorption axis of the analyser. The polarisation state of the light will rotate to *H* along path L_4 on the circle *j* by passing through the +*C*-plate, and, finally, the polarisation state will reverse-rotate to *J* along path L_5 on

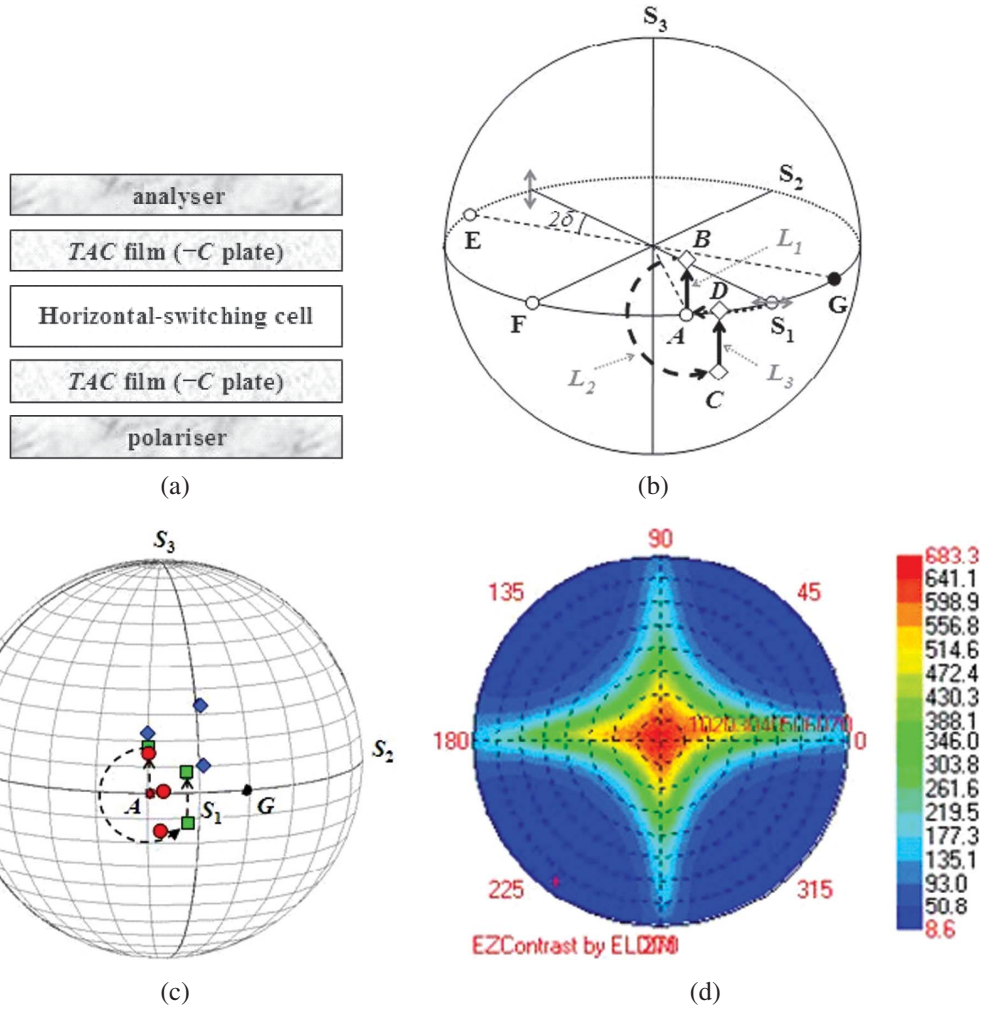

Figure 1. (Colour online). Conventional transmissive IPS LC cell: (a) optical structure; (b) polarisation path on the Poincaré sphere; (c) calculated polarisation states of the light for the red, green and blue wavelengths; (d) measured iso-contrast.

the circle *j* because the TAC film exhibits negative birefringence. Finally, position *J* is exactly matched with the opposite position of the polarisation state of the analyser *E*. The process of advanced optical configuration effectively moves to the polarisation position of the output polarisers in the oblique incident direction, so that it clearly provides blocking of light leakage in the dark state.

However, for the best dark state we should consider phase dispersion of the LC cell, because the advanced configuration should satisfy the above principle along the range of the entire wavelength so that we need to optimise the retardation value of the two *A*-plates and a single +*C*-plate. Elimination of phase dispersion represents the coincidence of the polarisation state between *R*, *G*, *B* wavelengths on the Poincaré sphere in front of the output polariser.

Figure 2(c) shows the optical principle of the advanced horizontal-switching cell to remove the phase dispersion through the wavelengths *R*, *G* and *B* on the Poincaré sphere (*12*). In order to gather the polarisation positions on the entire wavelength to position *J*, we have to satisfy two conditions as below. The first is that the polarisation positions of the each wavelength passing through the upper *A*-plate should be on the circle *j* as shown in positions G_b, G_g and G_r in Figure 2(c). The subscript of the letter for each position represents the position of each *R*, *G* and *B* wavelength. The aligned polarisations of the entire wavelength on the circle *j* can be gathered by adjusting the retardation of the upper +*C*-plate. The second condition to optimise is to control the retardation of the +*C*-plate to the same phase dispersion of the TAC film before the light passes the TAC film. Optical calculations for satisfying the two conditions

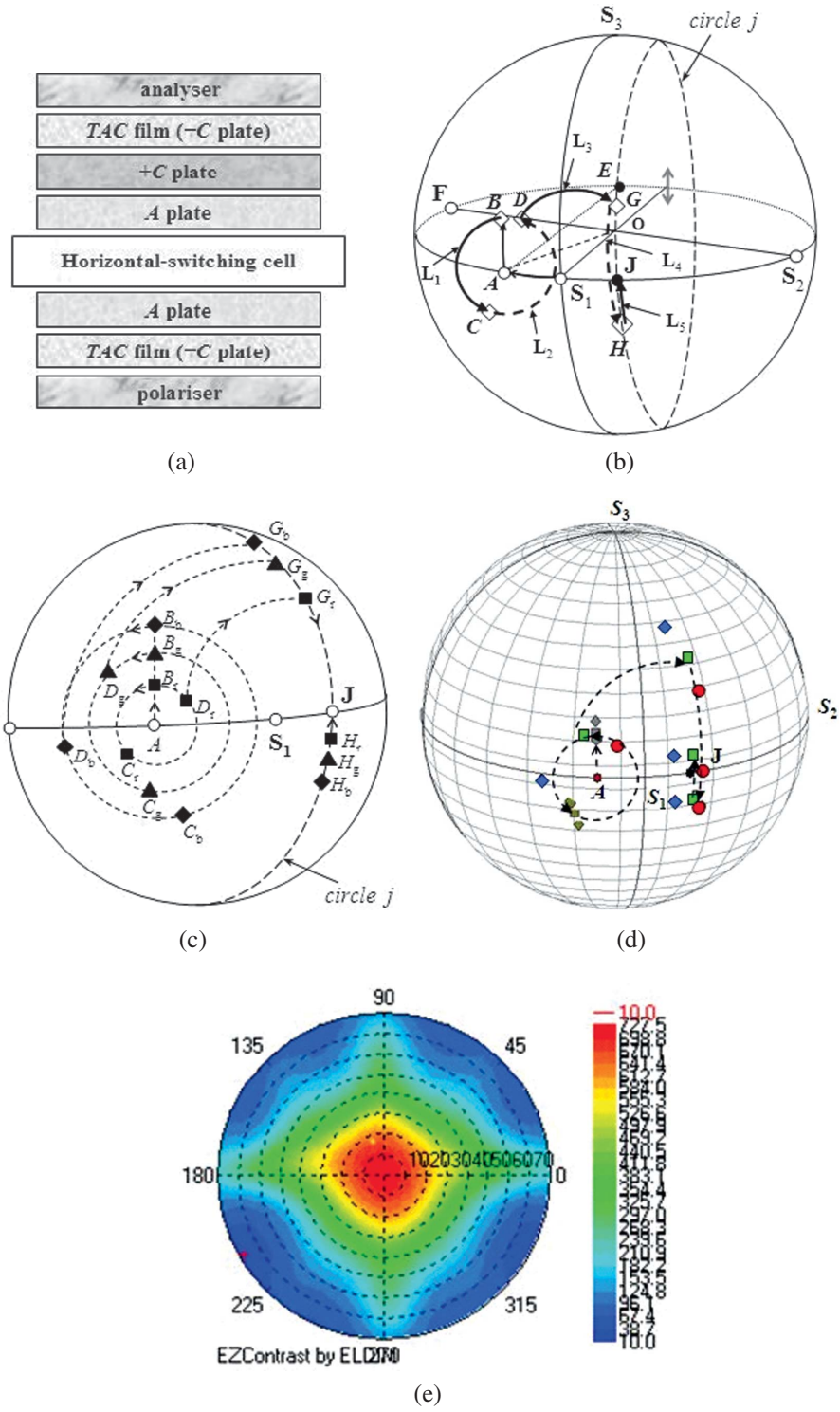

Figure 2. (Colour online). Advanced transmissive IPS LC cell with two *A*-plates and one *C*-plate: (a) optical structure; (b) polarisation path on the Poincaré sphere; (c) polarisation path for the red, green and blue wavelengths; (d) calculated polarisation states of the light for the red, green and blue wavelengths; (e) measured iso-contrast.

can be geometrically calculated on the Poincaré sphere (*12*, *15*). Figure 2(d) represents the calculated polarisation state of the *R*, *G*, *B* wavelengths when the light passes through the optical components in the advanced LC cell. Figure 2(e) represents the measured iso-contrast contour of the advanced LC cell, which can show a wider viewing angle compared with the conventional LC cell (*12*).

3.3 Advanced optical configuration using one A-plate and two C-plates for the transmissive IPS LC cell

The optical configuration of the advanced LC cell consists of a horizontal-switching LC cell with half-wave retardation, two *C*-plates, an *A*-plate and crossed polarisers coated with TAC film that has no retardation, as shown in Figure 3(a) (*16*). In this configuration, the *A*-plate is aligned perpendicular to the absorption axis of the input polariser between the LC cell and the upper *C*-plate. The polarisation path of the advanced LC cell for the dark state can be also described on the Poincaré sphere as shown in Figure 3(b) (*16*). From the start position *A* in the oblique incidence, the polarisation of the light passing through the lower *C*-plate moves to position B_i along circle path L_1, which is centred at position *F*. The subscript *i* represents the wavelengths *R*, *G*, and *B*. Then, the polarisation of the light approaches position C_i along circle path L_2 by the LC cell, which is centred at position *P*. Next, the polarisation state rotates to D_i on circle *e* along path L_3 by passing through the upper *A*-plate, which is centred at position *A*. Finally, the polarisation state will rotate to position *E* along path L_4 on the circle *e* by passing through the upper

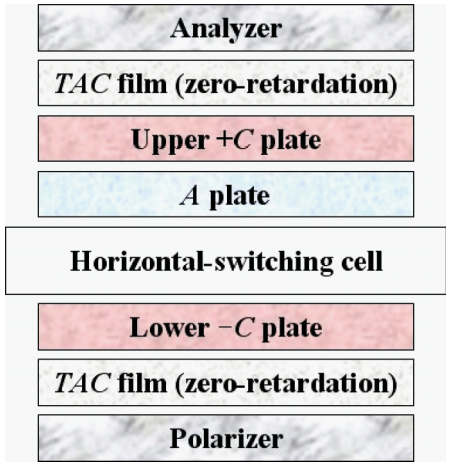

(a)

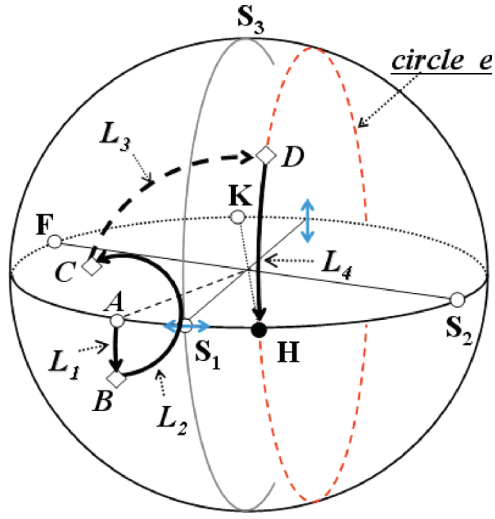

(b)

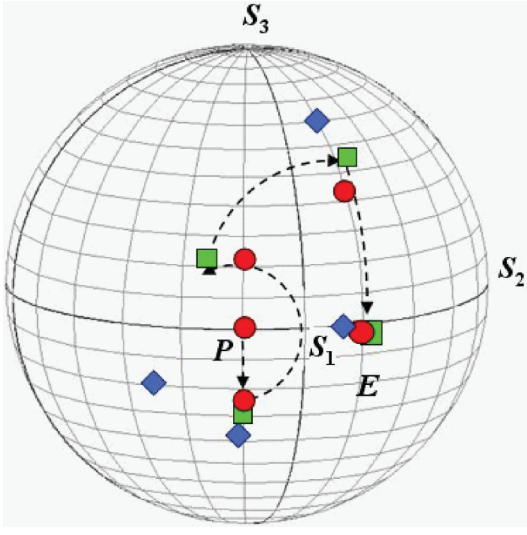

(c)

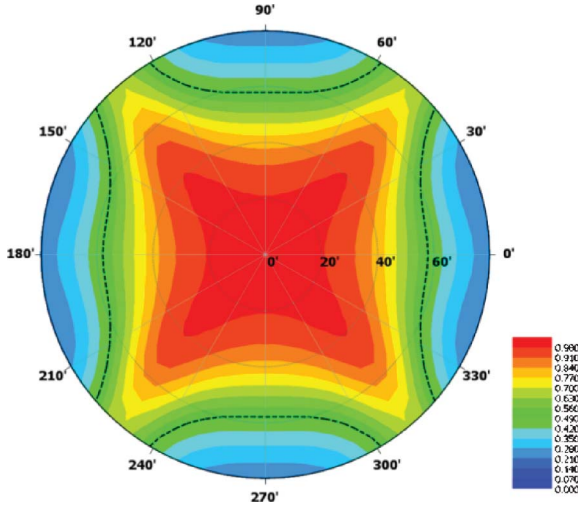

(d)

Figure 3. (Colour online). Advanced transmissive IPS LC cell with one *A*-plate and two *C*-plates: (a) optical structure; (b) polarisation path on the Poincaré sphere; (c) calculated polarisation states of the light for the red, green and blue wavelengths; (d) calculated iso-contrast.

C-plate. Position *E* is adjusted to exactly the opposite position of polarisation position *A*, which is the position of the output polariser. Therefore, it can block light leakage in the dark state.

In order to get an excellent dark state, polarisation of the entire wavelength should gather at point *E* in the same way as shown in Figure 3(b) (*16*). In particular, gathering the polarisation positions along all wavelengths to position *E* can be performed by optimising the phase dispersion of the lower *C*-plate and the *A*-plate so that the polarisation state of all wavelengths are on circle *e*, as shown in Figure 3(b). Finally, gathering the light's polarisation states at position *E* is done by optimising the upper *C*-plate's phase dispersion. The process for optimising the phase dispersion of the retarders to get an excellent dark state can be also calculated by the trigonometric method on a Poincaré sphere (*15, 16*). Figure 3(c) represents the calculated polarisation path of the *R, G, B* wavelengths in the advanced LC cell. Figure 3(d) represents the calculated iso-contrast contour of the advanced LC cell, which can also show a wide viewing angle compared with the conventional LC cell (*16*).

4. Transmissive vertical alignment liquid crystal mode

4.1 Polarisation states for the conventional transmissive VA LC cell

The conventional vertical alignment LCD consists of a VA LC cell and two TAC films on the crossed polarisers, as shown in Figure 4(a) (*17*). Figure 4(b) shows the polarisation state of the light obliquely passing through the cell in the diagonal direction on the Poincaré sphere (*17*). Like the conventional IPS LC cell, the start position in the oblique incidence ($\theta = 70^\circ$ and $\phi = 45^\circ$) on the Poincaré sphere is position *A*, deviated by 2δ from S_1, when the light passes through the polariser. The polarisation state passing through the lower TAC film with slow axis *OF* has polarisation position *B* along the circle path L_1. Next, the polarisation state of the light will move to position *C* along the circle path L_2 by experiencing the vertically aligned LC cell. Finally, the upper TAC film will move the polarisation state to position *D* from the position *C* with path L_3. From Figure 4(b) we can observe that the polarisation position is quite different from the polarisation position *D* in front of the output polariser *H,* so that the deviation between position *D* and position *H* will cause serious light leakage in the dark state.

Figure 4(c) represents the calculated polarisation path of the *R*, *G*, and *B* wavelength light on the Poincaré sphere in front of the output polariser at $\phi = 45^\circ$, $\theta = 70^\circ$. Figure 4(d) represents the calculated iso-contrast of the conventional VA LC cell, which exhibits a very narrow viewing angle (*18*).

4.2 Advanced optical configuration using two A-plates and two C-plates for the transmissive VA LC cell

Figure 5(a) shows the advanced optical configuration of the VA LC cell, which can improve the viewing angle in all directions (*17*). The optical configuration of the advanced LC cell is composed of two *A*-plates, two *C*-plates, and a vertical alignment LC cell. We have assumed that the optical axis of the VA LC layer in the absence of an electric field is the same as the optical axis of *C*-plate. The optical axis of the lower *A*-plate is aligned with the transmission axis of the incident polariser, and the optical axis of the upper *A*-plate is aligned along that of transmission axis of the analyser. An improved optical polarisation path of the advanced LC cell is described on the Poincaré sphere as shown in Figure 5(b) (*17*).

By using the optical configuration, the polarisation state in front of the output polariser can be coincided with the absorption axis of the analyser through seven optical paths (L_1 to L_7) by each optical component. The polarisation of the light passing through the lower TAC film and positive *C*-plate moves to position *C* along the circle path L_1 and L_2, which is centred at the same point *Q*. The polarisation of the light approaches position *D* along the circle path L_3 after passing through the lower positive *A*-plate with the optical axis *OA*. Then the polarisation of the light passing through the upper *A*-plate moves to position *E* along the circle path L_4 because the optical axis of the upper *A*-plate is aligned parallel with the absorption axis of the analyser. The next polarisation state of the light after passing through the VA LC cell with fast axis *OQ* will rotate to position *F* along path L_5. Finally, the polarisation state passing through the negative *C*-plate and upper TAC film reversely rotates to proceed to the position *H* by way of the position *G* along path L_6 and L_7. Position *H* is exactly matched with the opposite position *K* of the polarisation state of analyser. The process of the advanced optical configuration effectively moves the polarisation positions to the polarisation position of the analyser for the oblique incident direction, so that it clearly eliminates the off-axis light leakage in the dark state.

The phase dispersion of the LC cell is the next step to be considered because the advanced configuration should satisfy the above principle along the range of the entire visible wavelength. Elimination of the phase dispersion represents the coincidence of the polarisation states among *R*, *G*, and *B* wavelengths on the Poincaré sphere in front of the output polariser. Optical calculations for the optimisation of the used retardation films were calculated on the Poincaré sphere by using the Stokes vector and Muller matrix

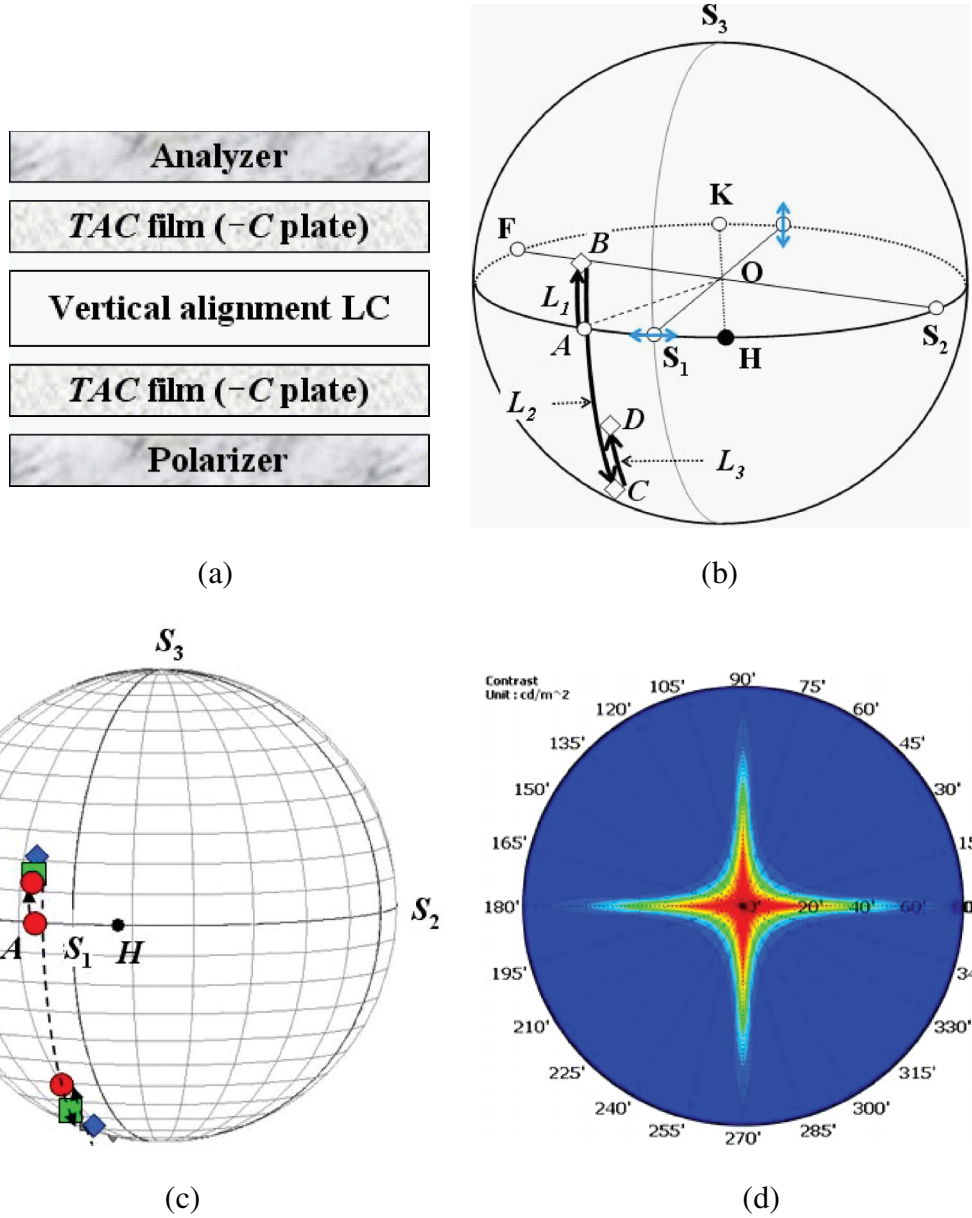

Figure 4. (Colour online). Conventional transmissive VA LC cell: (a) optical structure; (b) polarisation path on the Poincaré sphere; (c) calculated polarisation states of the light for the red, green and blue wavelengths; (d) calculated iso-contrast.

method (*17*). Figure 5(c) represents the calculated polarisation state of the *R*, *G*, *B* wavelengths when the light passes through the optical components in the advanced LC cell. Figure 5(d) represents the calculated iso-contrast contour of the advanced LC cell, which can show a wider viewing angle compared to the conventional VA LC cell.

4.3 Advanced optical configuration using one A-plate and two C-plates for the transmissive VA LC cell

Figure 6(a) shows another optical configuration of the advanced LC cell with a combination of a positive *A*-plate, a positive *C*-plate and a negative *C*-plate (*18*). The optical axis of the *A*-plate is aligned with the absorption axis of the incident polariser. An improved polarisation path of the advanced LC cell can be described on the Poincaré sphere, as shown in figure 6(b) (*18*).

The polarisation state of the light passing through the positive *C*-plate moves to position *B* along the circle path L_1, centred at the point *F*. The polarisation position of the light moves to position *C* along the circle path L_2 passing through the positive *A*-plate, which has a position *K* for the optical axis. Then, polarisation of the light passing through the VA LC layer moves to position *D* along circle path L_3 with a

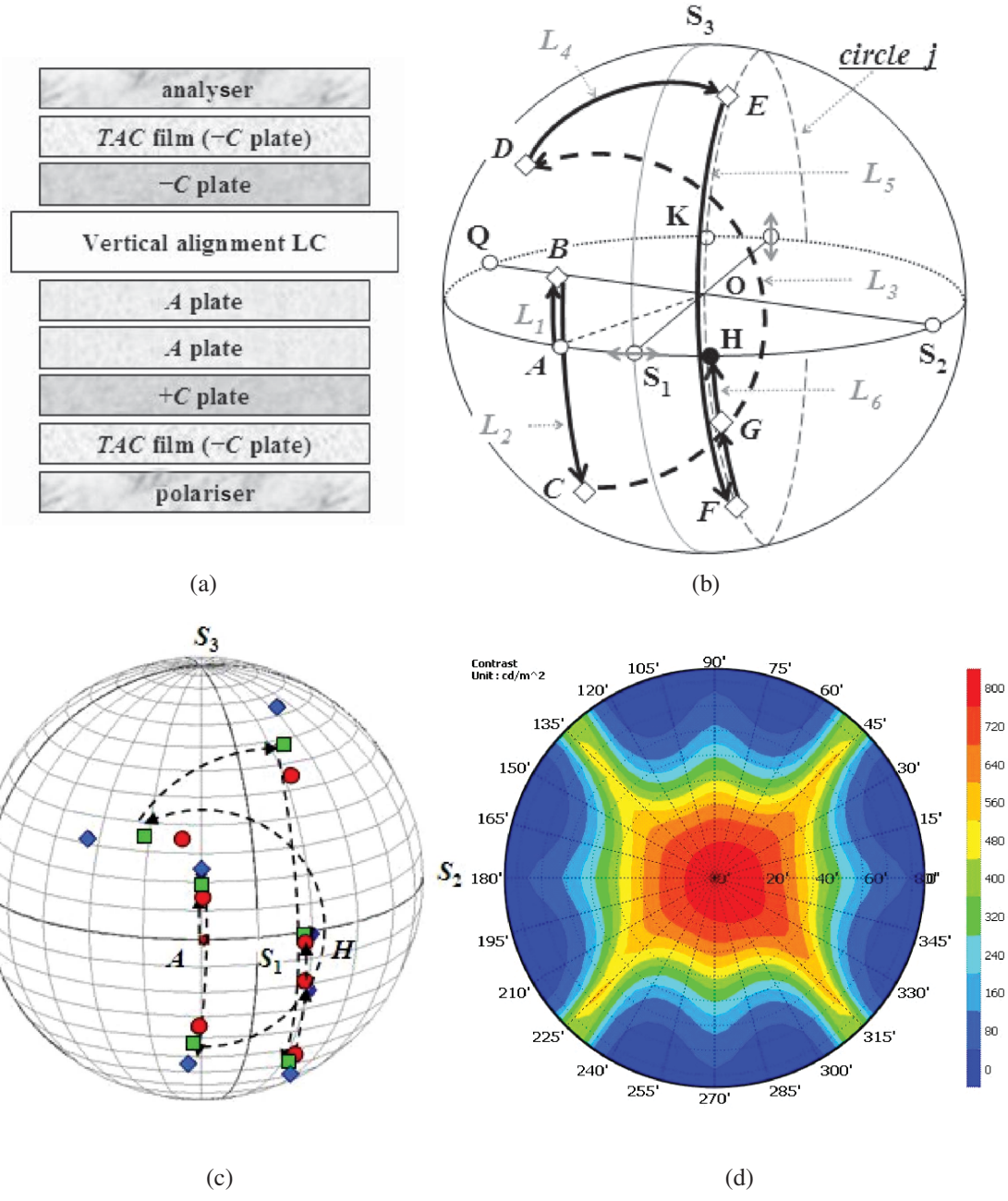

Figure 5. (Colour online). Advanced transmissive VA LC cell with two *A*-plates and two *C*-plates: (a) optical structure; (b) polarisation path on the Poincaré sphere; (c) calculated polarisation states of the light for the red, green and blue wavelengths; (d) calculated iso-contrast.

centred position *F*. Finally, the polarisation state of the light passing through the negative *C*-plate reversely rotates to proceed to position *H* along path L_4. The position *H* in front of the analyser is exactly matched to the opponent position *K* of the analyser. Therefore, the process of the advanced optical configuration can effectively move the polarisation position of the light passing through the cell to the desired position, which should be the opponent position of the polarisation axis of the analyser in the oblique incidence so that it can clearly eliminate the off-axis light leakage in the dark state.

For the perfect achromatic black state, we optimised the retardation value of the compensation films to gather the polarisation positions of the entire visible wavelength to position *H* (*18*). Figure 6(c) represents the calculated polarisation state of the *R*, *G*, *B* wavelengths when the light passes through the optical

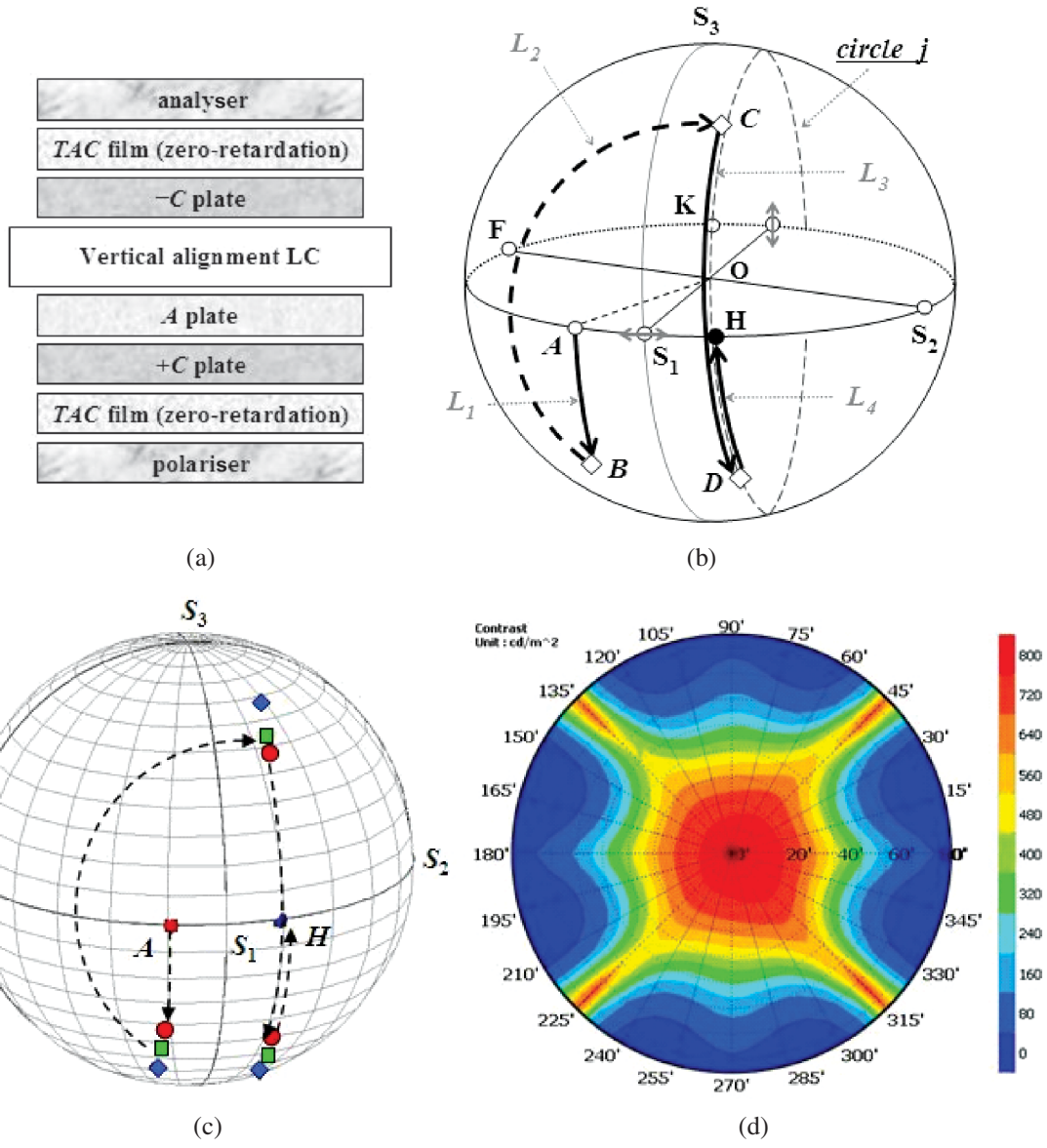

Figure 6. (Colour online). Advanced transmissive VA LC cell with one *A*-plate and two *C*-plates: (a) optical structure; (b) polarisation path on the Poincaré sphere; (c) calculated polarisation states of the light for the red, green and blue wavelengths; (d) calculated iso-contrast.

components in the advanced LC cell. Figure 6(d) represents the calculated iso-contrast contour of the advanced LC cell, which can show wider viewing angle compared to the conventional LC cell (*18*).

5. Reflective in-plane switching liquid crystal mode

5.1 Polarisation states for the conventional reflective IPS LC cell

The conventional reflective IPS LC cell is sequentially stacked by a polariser, a half-wave retarder and a quarter-wave LC cell and a reflector, which has been presented in the previous paper, as shown in figure 7(a) (*19*). Figure 7(b) and (c) explains the light leakage in the dark state on the Poincaré sphere. Figure 7(b) shows the principle of the compensation of the phase retardation for the wideband property in the normal direction (*19*). Polarisation paths L_1 by the half-wave retarder and L_2 by the quarter-wave LC layer effectively compensate for the phase dispersion along the full visual wavelength range, so that all the polarisation positions of all the wavelengths proceed to position S_3 in front of the mirror. Positions *A*, *B* and *C* in Figure 7(b) represent the polarisation position of the polariser, the half-wave retarder and the quarter-wave LC cell, respectively.

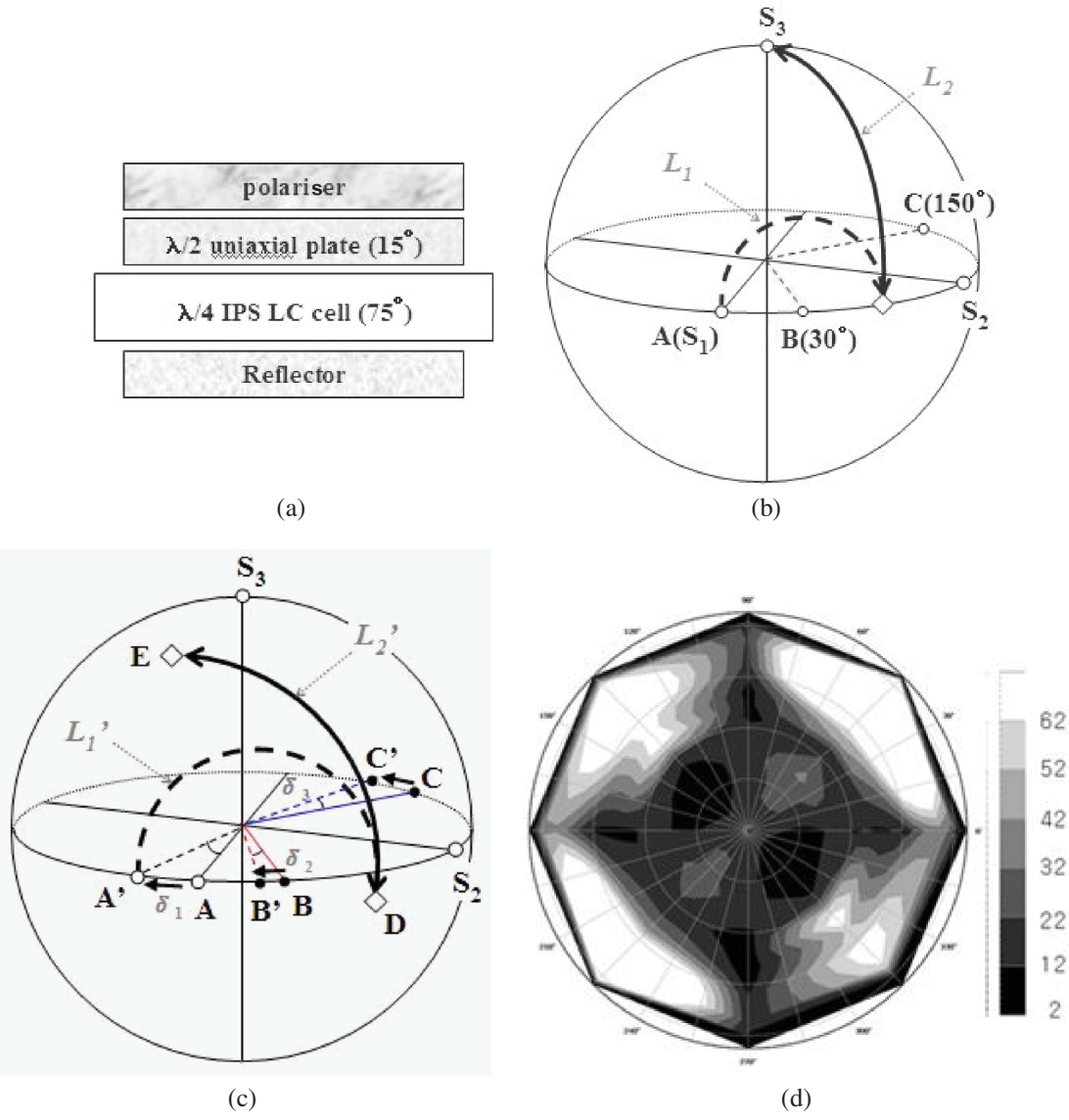

Figure 7. (Colour online). Conventional reflective IPS LC cell: (a) optical structure; (b) polarisation path in the normal direction on the Poincaré sphere; (c) polarisation path in the diagonal direction on the Poincaré sphere; (d) calculated iso-luminance in the dark state.

On the contrary, the polarisation path of all the wavelengths in the oblique direction in the oblique direction may not proceed to S_3, as shown in Figure 7(c) (*19*). In the oblique incidence, the polarisation axis of the polariser and the optical axis of each optical film have the deviation angle δ from the normal direction. In Figure 7(c), δ_1, δ_2 and δ_3 represent the deviation angle of the polariser, the half-wave retarder and the quarter-wave LC layer, respectively. As a result, positions A, B and C move to the deviated positions A' ($= -2\delta_1$), B' ($= 30° - \delta_2$) and C' ($= 150° + \delta_3$), respectively. And path lengths L_1 and L_2 are also changed to L_1' and L_2' by the changed retardation of the each retardation layers. In the oblique direction, the polarisation of the light passing through the polarisation proceeds to A' with deviation angle δ_1. By passing through the half-wave retarder, the polarisation state of the light proceeds to position D with circle path L_1', which has centring position B'. The polarisation of the light passing through the quarter-wave LC layer proceeds to E with circle path L_2', which is centred at position C'. As a result, the polarisation of the light in front of the mirror obviously deviates to E from the desired destination S_3.

Figure 7(d) represents the measured iso-luminance for the conventional reflective IPS LC cell in the dark state, which shows a narrow viewing angle characteristic in the diagonal direction (*19*).

5.2 Advanced optical configuration using one C-plate and one λ/2 biaxial film for the reflective IPS LC cell

The optical configuration of the advanced LC cell consists of a positive *C*-plate, a quarter-wave LC layer and a half-wave biaxial film instead of the half-wave *A*-plate, as shown in Figure 8(a) (*20*). An improved optical polarisation path of the advanced LC cell is described on the Poincaré sphere, which can place the polarisation position of the light in front of the mirror on the S_3 position in the oblique incidence, as shown in Figure 8(b) (*20*). First is that polarisation of the light passing through the biaxial film and the LC layer should be on the circle path L_3, which is centred at position *F* of the slow axis of the *C*-plate. Then, the optimised retardation of the positive *C*-plate can make the polarisation state of the light *E* proceed to S_3 with circle length l_4. The optical configuration is optimised in the diagonal and horizontal directions (ϕ = 45°, 0°) with polar angle θ = 70° at wavelength λ = 550 nm. In order to satisfy the first condition, we calculated the polarisation position of the light as a function of parameter N_z (= (n_x - n_z)/ (n_x - n_y)) after the light passes through the half-wave biaxial film and the quarter-wave LC cell.

Figure 8(c) represents the measured iso-luminance contour of the advanced reflective LC cell, which can show wider viewing angle compared with the conventional LC cell (*20*).

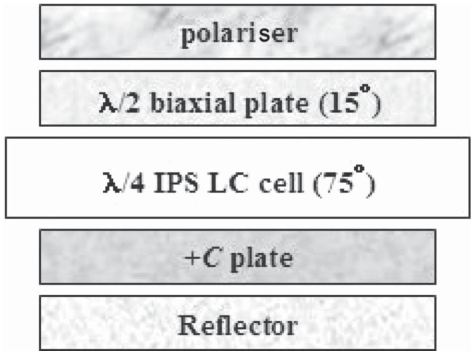

(a)

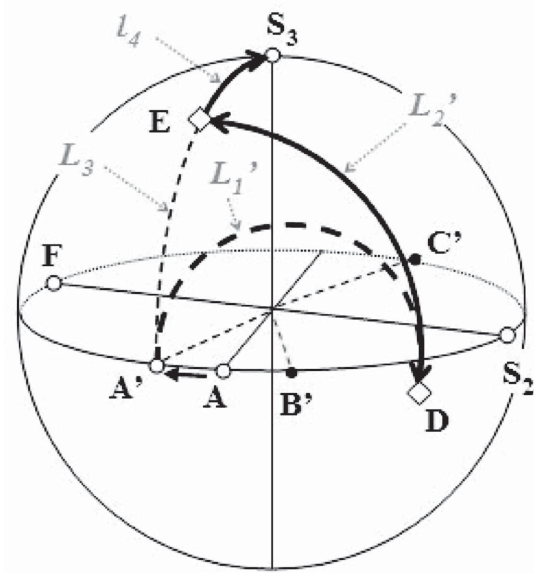

(b)

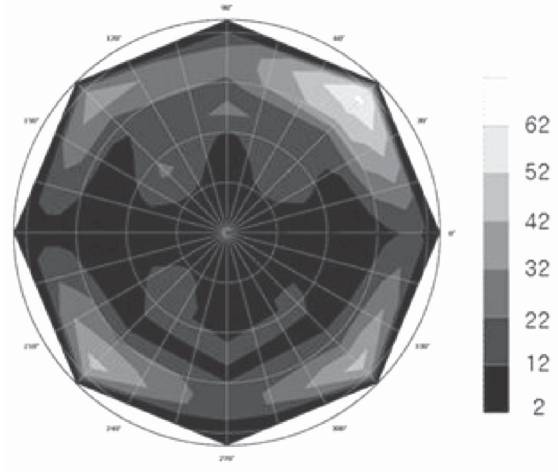

(c)

Figure 8. (Colour online). Advanced reflective IPS LC cell: (a) optical structure; (b) polarisation path on the Poincaré sphere; (c) calculated iso-luminance in the dark state.

6. Conclusions

We have introduced the advanced optical configurations with improved viewing angle and contrast ratio for the transmissive and reflective LCDs. The trace of the polarisation changes was demonstrated on the Poincaré sphere in a visible wavelength range. Optical compensation to eliminate the off-axis light leakage in the dark state was performed on the Poincaré sphere by using the trigonometric and the Muller matrix method. By optimising the wavelength dispersion of used optical retardation films, we could control the wide-view characteristics for the IPS and VA LC mode in the transmissive and reflective LCDs.

Acknowledgements

This paper was supported by Dong-A University Research Fund in 2009.

References

(1) Oh-e M.; Kondo K. *Appl. Phys. Lett.* **1995**, *67*, 3895–3897.
(2) Lee S. H.; Lee S. L.; Kim H. Y. *Appl. Phys. Lett.* **1998**, *73*, 2881–2883.
(3) Kim K. H.; Lee K. H.; Park S. B.; Song J. K.; Kim S. N.; Souk J. H. In *18th Int. Display Research Conf.* (*Asia Display'98*) **1998**; pp 383–386.
(4) Ohmuro K.; Kataoka S.; Sasaki T.; Koike Y. *SID Dig. Tech. Papers* **1997**, *28*, 845–848.
(5) Ogawa T.; Fujita S.; Iwai Y.; Koseki H. *SID Dig. Tech. Papers* **1998**, *29*, 217–220.
(6) Wu S.-T.; Wu C.-S.; Kuo C.-L. *J. Soc. Information Display* **1999**, *7*, 119–126.
(7) Ishinabe T.; Miyashita T.; Uchida T. *Jpn. J. Appl. Phys.* **2002**, *45*, 4553–4558.
(8) Yeh P.; Gu C. *Optics of Liquid Crystal Displays*; Wiley, 1999.
(9) Zhu X.; Ge Z.; Wu S.-T. *J. Disp. Tech.* **2006**, *2*, 2–20.
(10) Yang D.-K.; Wu S.-T. *Fundamentals of Liquid Crystal Devices*; Wiley, 2006.
(11) Fujimura Y.; Kamijo T.; Yoshimi H. *SPIE*, **2003**, *5003*, 96–105.
(12) Lee J.-H.; Choi H. C.; Lee S. H.; Kim J. C.; Lee G.-D. *Appl. Opt.* **2006**, *45*, 7279–7285.
(13) Bigelow J.E.; Kashnow R.A. *Appl. Opt.* **1977**, *16*, 2090–2096.
(14) Vermeirsch K.; Meyere A.D.; Fornier J.; Vleeschouwer H.D. *Appl. Opt.* **1999**, *38*, 2775–2786.
(15) Goldstein D. *Polarized Light*; CRC Press, 2003.
(16) Lee J.-H.; Son J.-H.; Choi S.-W.; Lee W.-R.; Kim K.-M.; Yang J.-S.; Kim J.C.; Choi H.C.; Lee G.-D. *J. Phys. D: Appl. Phys.* **2006**, *39*, 5143–5148.
(17) Ji S.-H.; Lee G.-D. *J. Info. Disp.* **2008**, *9*, 22–27.
(18) Ji S.-H.; Lee S.H.; Lee G.-D. *Appl. Opt.* **2009**, *48*, 48–54.
(19) Yoon T.-H.; Lee G.-D.; Kim J.C. *Opt. Lett.* **2000**, *25*, 1547–1549.
(20) Ko T.W.; Kim J.C.; Choi H.C.; Park K.-H.; Lee S.H.; Kim K.-M.; Lee W.-R.; Lee G.-D. *Appl. Phys. Lett.* **2007**, *91*, 053506.